RSC Advances

ROYAL SOCIETY OF CHEMISTRY

www.rsc.org/advances

Journal Name

RSCPublishing

ARTICLE

Effect of Polymer Stereoregularity on Polystyrene/Single-Walled Carbon Nanotube Interactions

Cite this: DOI: 10.1039/xoxxoooooox

Received ooth January 2012,
Accepted ooth January 2012

DOI: 10.1039/xoxxoooooox

www.rsc.org/

L. A. London,[a] L. A. Bolton,[a] D. K. Samarakoon,[a] B. S. Sannigrahi,[a] X. Q. Wang,[b*] and I. M. Khan[a]

We use a combination of computational and experimental studies to elucidate the effect of polymer stereoregularity on the capability of polystyrene interacting with single-walled carbon nanotube (SWNT) surfaces. Calculated binding energies on complexes of lightly oxidized SWNT with isotactic and atactic polystyrene favor the former, which suggests that the isotactic polymer interacts more effectively with the SWNT. The glass transition temperature (T_g) of the isotactic polystyrene/SWNT matrix increases from 90.9 to 100.5 ^{o}C as the SWNT content is increased to 0.5%, whereas the glass transition temperature of the atactic polystyrene/SWNT matrix is invariant with increasing SWNT content. Rotating frame ^{13}C $T_{1\rho}$ relaxation rates for the isotactic polymer/SWNT matrix increases from 2.15 to 2.43 ms as SWNT is increased from 0.25 to 1.0 %. However, the rotating frame ^{13}C $T_{1\rho}$ relaxation rates for the atactic polymer/SWNT matrix decreases from 2.50 to 1.60 ms as SWNT is increased from 0.25 to 1.0 %. Our results demonstrate that the SWNT is better dispersed within the isotactic polystyrene and the better dispersion is associated with more effective interaction of isotactic polymer with the SWNT surface.

Introduction

An innovative approach to developing new materials is by the incorporation of nanoparticles within a polymer matrix.[1-16] The overall property enhancements of the polymer along with the development of new and unique properties are possible because of not only the presence of the nanoparticle, but also the goodness of the dispersion of the particles within the matrix.[17-19] Strong polymer-nanoparticle interaction permits good dispersion, while weak interaction results in aggregation even at low contents. An interesting nanofiller is single-walled carbon nanotube (SWNT). The interest in SWNT as the nanofiller is attributed to its unique mechanical and electrical properties. Specifically, the high aspect ratio of SWNTs permits desired property enhancements at very low concentrations. Nanocomposites composed of SWNT and polystyrene (PS) have been reported by several groups.[20-24] Electrically conductive composites with excellent properties have been obtained with SWNT loadings lower than 1 wt%.[20-24] SWNTs normally agglomerate into bundles within polymer matrices and thus the dispersion of SWNTs requires effective tailoring of SWNT-polymer interactions.[25-30] Polystyrene/poly(2-methoxystyrene)/SWNT nanofibers decorated with functional groups can be utilized as sensors for model protein.[31-37] A fundamental question arises as to whether it is possible to tune the interaction between the polymer and the SWNT surface by utilizing the same polymer but with different stereoregularity. Polymer stereoregularity is a fundamental three-dimensional characteristic for most vinyl polymers. Polymers such as polystyrene, poly(methylmethacrylate), poly(vinylchloride), poly(propylene) and others can be classified as atactic, isotactic or syndiotactic polymers.[31] Atactic polymers have approximately equal meso (isotactic like) and racemo (syndiotactic like) dyads content in the polymer chain. By contrast, the meso and the racemo dyads are randomly distributed in the polymer chain. The spatial orientations of the meso and racemo dyads are shown in Figure 1. All the dyads are meso and raceme for a purely isotactic and syndiotactic polymer, respectively.

Stereoregularity can have a profound effect on the conformation of polymers and physical properties.[32-36] For example, syndiotactic poly(methylmethacrylate) has a glass transition temperature of 105 °C and that of the isotactic polymer is around 40 °C.[31] Isotactic polystyrene forms a helical conformation in the solid state.[38] The helical conformation is either in the extended helical conformation with a non-staggered trans-trans conformation, or three fold helical trans-gauche conformation. The conformation of isotactic polystyrene in the solid state is substantially different from the atactic polystyrene. As such, the stereoregularity and the associated conformation may affect the nature of the interaction between the polymer and SWNT with diameters around 1 nm. Composites of syndiotactic polystyrene and carbon nanofibers (CNF) with

diameters between 40-140 nm prepared by melt blending at 290 ^{0}C have been reported.[37-38] To understand the effect of polystyrene stereoregularity, it is necessary to use SWNT with smaller diameters.

In this paper, we report a combined approach of computational modelling and experimental studies to determine the interaction between atactic or isotactic polystyrene with the surface of SWNT. A careful examination of the results for isotactic polystyrene/SWNT matrix and atactic polystyrene/SWNT matrix provides a direct and controlled comparison of the efficiency of their interaction with SWNTs.

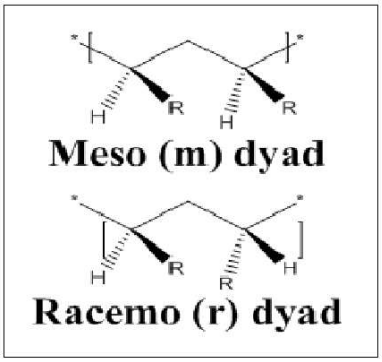

Figure 1. Meso and racemo dyads of polystyrene.

Experimental

Materials

SWNT material in the form of a fibrous powder with chirality (7, 6) and diameter range 0.7-1.3 nm was purchased from Sigma-Aldrich Co. LLC, St. Louis, MO. Syndiotactic and isotactic polystyrene was purchased from Scientific Polymer Products Inc., Ontario, NY. Isotactic polystyrene was obtained in powder form having an MW of 4×10^5 grams/mol with a reported tacticity of greater than 90%. Atactic polystyrene was obtained from Aldrich and had a reported MW of 4.4×10^4 grams/mol. All other materials were purchased from Sigma-Aldrich and used as received.

Preparation of the Oxidized SWNT

Preparation of oxidized SWNT: SWNT was lightly oxidized by nitric acid by the method reported in literature.[39] Raman spectroscopy was used to obtain the percent oxidation of the functional tubes used in composite formation.[39-40] The percent oxidation was calculated according to the following equation:

$$\frac{I_D}{I_G} \times 100\%, \qquad (1)$$

where I_D is the D-band integration at 1300 cm^{-1} and I_G is the G-band integration at 1590 cm^{-1}. Comparing pristine tubes to nitric acid oxidized tubes, the degree of functionalization was found to be approximately 6%.

Preparation of SWNT-Polystyrene Matrices

A bath-sonicated dispersion of lightly oxidized SWNTs was centrifuged and washed in 10 mL distilled H_2O and 10 mL MeOH several times. The SWNT was re-dispersed in 20 mL of dimethyl formamide (DMF) and bath sonicated for 60 min. Separate solutions each containing 100 mg of isotactic and atactic polystyrene were dissolved in DMF, allowed to stir overnight, and sonicated for 60 min. The isotactic PS was pre-dissolved in THF for facile processing. To prepare the matrices, each PS solution was mixed with a SWNT solution containing 0.25, 0.5, 1, 2, 3 or 5% mass of SWNTs relative to PS mass. Each sample was allowed to stir 60 min, sonicated for 60 min, and then stirred overnight. The samples were precipitated in 10-fold excess H_2O stirring vigorously, filtered using PTFE membrane, washed with H_2O and MeOH, and then dried at 110°C for one hour.[40]

Carbon $T_{1\rho}$ Relaxation

Rotating frame carbon relaxation rates ($T_{1\rho}$) of solid samples were determined at room temperature in a 500 MHz Bruker AVANCE III NMR instrument at a spinning rate of 5 kHz with 5 mm Zirconium spinners. A 4 μs 90^o pulse sequence (p1) was employed followed by variable durations. Typically, the spin locking pulse sequence was applied ranging from 0.001 ms to 5 ms (16 different pulses) to the samples within the expected range of relaxation time. The value of pulse power was used for relaxation measurement purposes. The number of pulse sequences corresponded to the number of data points collected for the relaxation calculation. Relaxation data were directly fitted to a binomial equation using Bruker topspin analysis software.

Instrumentation

Ultrasonification was performed using a Fisher FS-30 160W Ultrasonicator. Differential scanning calorimetric analysis was conducted under nitrogen using a TA Instrument Q2000 with Tzero hermetically sealed lids and pans. Solution NMR spectra were obtained using a Bruker 500 MHz Bruker AVANCE III nuclear magnetic resonance spectrometer using deuterated solvent chloroform.

Sample Preparation and Measurement

For each pure polymer sample, ^{13}C NMR spectra were obtained in deuterated chloroform at room temperature using a solution of 3-5 mg of polymer in 0.75 ml of solvent. The 500 MHz ^{1}H-NMR spectra of SWNT-polymer solutions were also carried out in chloroform (deuterated) at room temperature. The changes in chemical shift for the aromatic protons of the polystyrene as a function of SWNT were determined relative to the chloroform peak at 7.29 ppm. Each sample was run three times and the average change in chemical shift was determined. Pure polymer samples and polymer/SWNT matrices were placed in DSC Tzero pans as a thin layer of powder for equal distribution. To produce good sample-pan contact, a pre-melt step was ramped up to 250°C, held for five minutes and cooled at 30°C per minute. Only 1-2 runs were necessary to reach a limiting constant value for the T_g. The glass transition temperature from the third run is reported. For all samples, the sample sizes did not exceed 3-5 mg. Glass transition temperature and changes in heat capacity (ΔC_p) measurements were obtained using steps previously reported[40] using a heating rate of 10°C/min and cooling of 60°C/min from a fully melted sample.

Computational Methods

First-principles calculations based on dispersion-corrected DFT was employed to describe interactions between the polystyrene and SWNTs. Perdew–Burke–Ernzerhof (PBE) parameterization of exchange correlation was used with a double numerical with polarization function (DNP) basis set as implemented in DMol3.[41] The general gradient approximation (GGA) results were subsequently rectified through the inclusion of a dispersion correction effect. Tkatchenko–Scheffler (TS) dispersion correction accounts for the relative variation in dispersion coefficients of differently bonded atoms by weighting values taken from the highly accurate *ab*-initio database with atomic volumes extracted from partitioning the self-consistent electronic density. The TS scheme exploits the relationship between polarizability and volume. The optimization of the atomic position was carried out with convergent forces less than 0.01 eV/Å. The change in the total energy was less than 3×10^{-4} eV per unit cell. The lightly oxidized SWNTs were based on epoxy conformations with 5% or 10% oxidization in order to facilitate the experimental situations. We used semiconducting (13,0) tubes in our calculations.

Results and Discussion

Calculations were performed on purely isotactic, atactic and syndiotactic polystyrene/SWNT complexes to determine which polymer has the stronger affinity for interacting with the surface of SWNT. Each polystyrene model was composed of twelve monomer units. The isotactic and syndiotactic models consisted of all meso or racemo dyads, respectively (Figure 1). The atactic polystyrene had a random distribution of meso and racemo dyads. Computational results demonstrate that the semi-rigid aromatic polystyrene backbone has certain flexibility to adjust its conformation during successive helical wrapping.[42-45] The initial sets of calculations were carried out using pristine SWNTs. The same calculation procedure and the parameters have been employed for three conformations (isotactic, atactic, and syndiotactic) of polystyrene-wrapped carbon nanotubes. The error associated with calculation is less than 1 kcal/mol. As such, energy change between isotactic and the other two conformations (atactic and syndiotactic) is about 8 kcal/mol. There is an energy difference of 1 kcal/mol between atactic and syndiotactic conformations.

Among the three tacticities shown in Figure 2, it was observed that isotactic polystyrene forms the lowest energy complex. The calculated binding energies (BE) listed in Table 1 revealed atactic/SWNT as the second most stable complex and the syndiotactic polystyrene/SWNT as the least stable. Therefore, the results suggest that the polymer with 100% meso (m) content is most effective in wrapping the SWNT, followed by the atactic polymer which has 50% meso (m) content and the syndiotactic polymer with 0% meso (m) content is least effective in wrapping the SWNT. This implies that the meso sequences in the polystyrene may be conformationally in a favorable state to form polymer/SWNT complexes with lower energies. The surface of SWNT is hydrophobic and inert in nature.[39-40] Previous experimental studies have shown that the interaction of SWNT with polystyrene can be improved by lightly oxidizing the SWNT. [39-40] Therefore, binding energies were also calculated for the interaction of polystyrene with lightly oxidized SWNT.

Binding energies of lightly oxidized SWNT with isotactic and atactic polystyrene complexes were -237.09 and -229.10 kcal/mol, respectively. The oxidation of SWNT further stabilized the interaction of the isotactic and the atactic polystyrene with the SWNT. Therefore, the calculated binding energies were consistent with the experimental observations.[36, 37] However, the oxidation of the SWNT has little influence on binding energy for the syndiotactic polymer/SWNT complex. Oxidation increases the polarity of the SWNT, resulting in an increase in the dipole-dipole interaction between the two components. The binding energy data suggest that the isotactic polystyrene is more effective in interacting with the SWNT. Hence, the stereoregularity of polystyrene plays a role in its ability to interact with the surface of the SWNT. A plausible explanation for this observation is that the isotactic polystyrene, which is 100% meso, forms an extended helical conformation, and the extended chain turns to be in a preferable conformation to start the wrapping around the SWNT. Furthermore, once the wrapping is completed, the wrapped polymer chain forms a lower energy conformation in the complex compared to the isotactic and the syndiotactic polymer. The predicted conformations for the lightly oxidized SWNT wrapped with atactic, isotactic and syndiotactic polystyrene are shown in Figure 2.

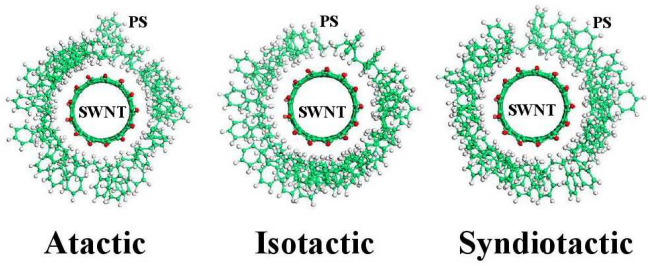

Figure 2. Predicted conformation for the lightly oxidized SWNT wrapped with polystyrene. (Red dots: oxygen atoms)

Binding energies of lightly oxidized SWNT with isotactic and atactic polystyrene complexes were -237.09 and -229.10 kcal/mol, respectively. The oxidation of SWNT further stabilized the interaction of the isotactic and the atactic polystyrene with the SWNT. Therefore, the calculated binding energies were consistent with the experimental observations.[36, 37] However, the oxidation of the SWNT has little influence on binding energy for the syndiotactic polymer/SWNT complex. Oxidation increases the polarity of the SWNT, resulting in an increase in the dipole-dipole interaction between the two components. The binding energy data suggest that the isotactic polystyrene is more effective in interacting with the SWNT. Hence, the stereoregularity of polystyrene plays a role in its ability to interact with the surface of the SWNT. A plausible explanation for this observation is that the isotactic polystyrene, which is 100% meso, forms an extended helical conformation, and the extended chain turns to be in a preferable conformation to start the wrapping around the SWNT. Furthermore, once the wrapping is

completed, the wrapped polymer chain forms a lower energy conformation in the complex compared to the isotactic and the syndiotactic polymer. The predicted conformations for the lightly oxidized SWNT wrapped with atactic, isotactic and syndiotactic polystyrene are shown in Figure 2.

Table 1. Calculated Binding Energies for Polystyrene/SWNT complex as a function of tacticity

Tacticity	[BE]Oxidized SWNT [kcal/mol]	[BE] Pristine SWNT [kcal/mol]
Isotactic	-237.09	-236.83
Atactic	-229.10	-228.97
Syndiotactic	-228.12	-228.12

Polystyrene Stereoregularity

The first-principles based dispersion-corrected DFT calculation results suggest that the isotactic polystyrene has the stronger interaction with the surface of the SWNT. Therefore, in order to validate the computational modelling predictions, pure isotactic and atactic polystyrene/SWNT matrices were experimentally studied by NMR and DSC methods. High molecular weight isotactic and atactic polystyrene were obtained from commercial suppliers. Before carrying out the studies, the stereoregularity of the two polymers were confirmed by ^{13}C NMR spectroscopy. The 125 MHz ^{13}C NMR spectra of the quaternary carbon of the isotactic and atactic polystyrenes are shown in Figure 3. The isotactic polymer displays one single peak at 146.2 ppm and the atactic polymer displays a set of overlapping peaks indicating at least pentad stereochemical resolution. The peak at 146.2 ppm observed for the isotactic polystyrene was assigned as the *mmmm* (or isotactic) pentad. Considering that only a single peak was observed for the quaternary carbon, it was concluded that the polymer was almost 100% isotactic.

The pentad stereochemical assignments for the atactic polymer are shown in Figure 4. The peaks were obtained by deconvolution of the quaternary peak shown in Figure 3. The assignments were made by comparison with the pure isotactic polymer and previously published stereochemical assignments.[46] The peak at 146.2 ppm was assigned to the *mmmm* pentad by comparing with the *mmmm* pentad peak of the isotactic polymer. The overall stereochemical assignments for the atactic polymer are listed in Table 2. The observed pentad intensities for the atactic polymer matched well with the intensities obtained by Bernoulli calculations, [47] also listed in Table 2. The Bernoulli calculations were performed using P_r value of 0.4. The P_r value was determined using the quaternary carbon *mmmm* pentad of the atactic polymer. The NMR analysis confirmed that the first polymer was a purely isotactic polystyrene and the second polymer was atactic polystyrene.

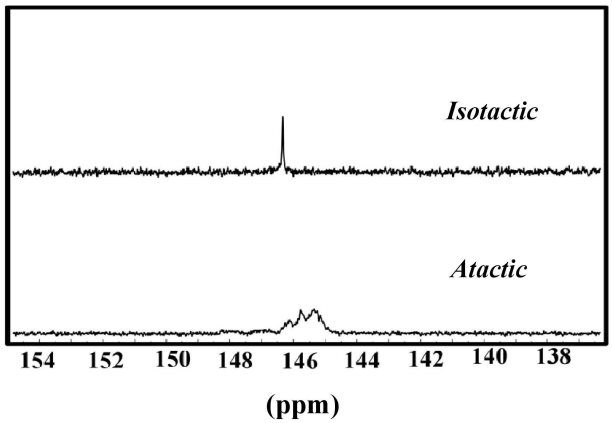

Figure 3. 500 MHz ^{13}C NMR spectra of the quaternary carbons of the isotactic and atactic polystyrenes.

Thermal Studies

The glass transition temperatures of the pure polymers and the polystyrene/SWNT matrices are listed in Table 3. The DSC thermograms of isotactic polystyrene/SWNT matrices are shown in Figure 5. The observed T_g values of the pure atactic-PS and isotactic-PS were in good agreement with previously reported values of ~100 and ~90°C, respectively.[46]

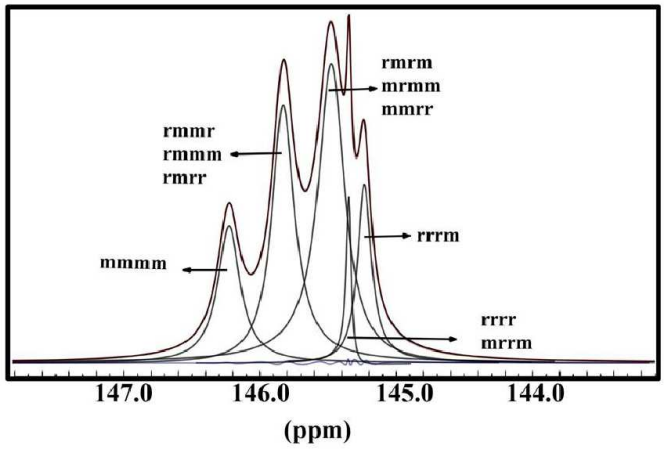

Figure 4. Pentad assignments of quaternary carbon peaks obtained by deconvolution.

The glass transition temperature of the atactic polystyrene decreases initially on adding SWNT and reaches a plateau with 0.5% weight SWNT content in the matrix. This observation is in conformity with an earlier observation reported by of Koning *et al*. that there is a slight decrease in T_g for PS-SWNT composites at low SWNT content.[48] The slight decrease in the T_g is attributed to the plasticization of the polymer by the SWNTs. As additional SWNT is added to the atactic polystyrene, larger agglomerates form and larger agglomerates do not affect the segmental motion of the polymer chains and thus the glass transition temperature is invariant. These

agglomerates can be viewed as small distinct domains, which do not significantly interact with the polystyrene chains. The fact that the SWNT do not interact with the polystyrene chains suggests that the interaction between the atactic polystyrene and the SWNT surface is weak.

Table 2. Stereochemical Assignments of Atactic Polystyrene Pentad Peaks

Peak Reg.	Chem. Shift (ppm)	Assignment	Observed Quaternary	P_R=0.4
A	146.2	*mmmm*	0.14	0.13
B	145.8	*rmmr*	0.29	0.31
		rmmm		
		rmrr		
C	145.5	*rmrm*	0.42	0.4
		mrmm		
		mmrr		
D	145.3	*rrrm*	0.04	0.08
E	145.2	*rrrr*	0.11	0.08
		mrrm		

The glass transition temperature of the atactic polystyrene decreases initially on adding SWNT and reaches a plateau with 0.5% weight SWNT content in the matrix. This observation is in conformity with an earlier observation reported by of Koning *et al*. that there is a slight decrease in T_g for PS-SWNT composites at low SWNT content.[48] The slight decrease in the T_g is attributed to the plasticization of the polymer by the SWNTs. As additional SWNT is added to the atactic polystyrene, larger agglomerates form and larger agglomerates do not affect the segmental motion of the polymer chains and thus the glass transition temperature is invariant. These agglomerates can be viewed as small distinct domains, which do not significantly interact with the polystyrene chains. The fact that the SWNT do not interact with the polystyrene chains suggests that the interaction between the atactic polystyrene and the SWNT surface is weak.

The isotactic polystyrene shows quite different thermal behavior. As the SWNT content is increased in the isotactic polymer, an increase in the T_g of the isotactic polystyrene/SWNT matrix is observed. The glass transition temperature quickly increases from 91°C to 100.5°C as the SWNT content is increased to 0.5%. Further increase in the SWNT content does not change the T_g. The initial increase in the glass transition temperature suggests that the isotactic polystyrene is better able to interact with the surface of the SWNT. Because the isotactic polystyrene effectively interacts with the SWNT, it is likely that two or more chains can simultaneously wrap the same SWNT particle, resulting in non-covalent crosslinking. The non-covalent crosslinking results in an increase in the glass transition temperature. Non-covalent crosslinking resulting in an increase in the glass transition temperature has been observed in certain polymer/salt systems because of ion-dipole interactions. [49-50] The DSC thermograms show some additional features**.** For example, i**n** the thermogram of the isotactic polystyrene containing **(F**igure 5d), we attribute the lower glass transition temperature around 90^0 C to the microphases of pure polystyrene and the higher one to the microphase of the polystyrene/SWNT matrix. Therefore, since t**he SWNT content is** small**,** ,it is quite likely, that the matrix will content microphase of pure polystyrene and a microphase of the polymer interacting with the SWNT i.e. a mic**r**ophase with a higher glass transition temperature.

Table 3. Glass transition Temperature (T_g) of the Pure Polymers and the Polystyrene/SWNT Nanocomposites

% SWNT	Atactic [°C]	Isotactic [°C]
0	102.9	90.9
0.25	98.3	98.4
0.5	99.8	100.5
1	99.5	100.2
2	98.9	100.8
3	100.1	99.9
5	99.8	100.4

The depiction of the addition of the SWNT to polystyrene is shown in Scheme 1.[51] Type A is pure polymer matrix. As SWNT is added to the polymer, if the polymer has good interaction with the SWNT, a Type B matrix is formed. In the Type B matrix, because the polymer interacts well with the SWNT, the SWNT is well dispersed throughout the matrix. Furthermore, in the Type B matrix since the polymer/SWNT forms well-defined complexes, these complexes possibly become sites where two or more chains can interact with the same SWNT particle, resulting in non-covalent crosslinking along with an increase in the glass transition temperature. We emphasize that the manner of interaction between the isotactic polymer and the SWNT is that short segments of the polymer chains will wrap/interact with SWNT i.e. short segments of multiple polymer chains can interact with one SWNT and this

is the reason that a SWNT can become a site for pseudo-crosslinking via non-covalent interaction resulting in an increase in the glass transition temperature. Further addition of SWNT to Type B matrix results in agglomeration of the SWNT as the capacity of the polymer to interact or complex with the nanofiller is saturated. Any additional SWNT past this point agglomerates and can be depicted by Type C matrix.

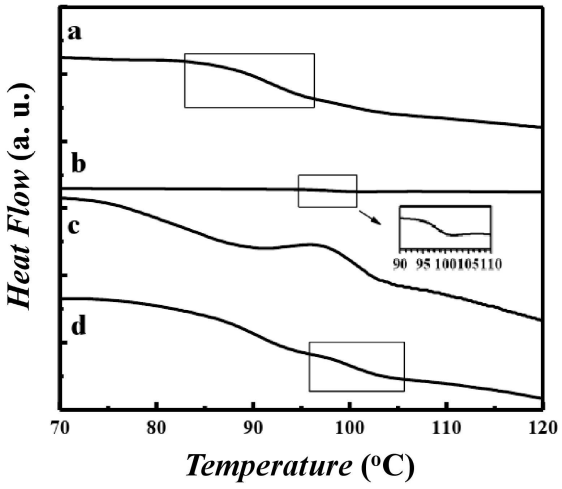

Figure 5. DSC thermograms of isotactic polystyrene/SWNT nanocomposites. a. Pure isotactic polystyrene, b. 0.25% SWNT, c. 1% SWNT, d. 0.5% SWNT.

Therefore, the additional SWNT, greater than past 0.5 to 5%, simply forms agglomerates, which do not interact with the polymer chains in that the glass transition temperature is unchanged. This is exactly the observation for the isotactic polystyrene/SWNT matrix. If the polymer does not interact well or complex effectively with the SWNT, even at low SWNT contents, the SWNT will most likely start aggregating and a Type D matrix will form. Therefore, a plasticization effect may be observed at low SWNT content. Further, increase in SWNT will result in agglomeration and hence after the initial plasticization, the glass transition will not be affected. This type of behavior is observed for atactic polystyrene/SWNT composite. From the thermal studies, one can conclude that the isotactic polystyrene interacts better and is more effective in complexing with the SWNTs compared with the atactic polystyrene. These observations are supported by the calculated binding energies listed in Table 1.

The magnitude of the ΔC_p at the glass transition temperature for the isotactic polystyrene/SWNT matrices increases as the SWNT content is increased. For the pure isotactic polystyrene the ΔC_p is 0.27 J/g°C. As the SWNT content is increased in the isotactic polymer matrix, the ΔC_p increases and reaches a value of 0.43 J/g°C at 1% by weight SWNT (Figure 6). The increasing change in the heat capacity suggests that at the glass transition temperature the segmental motion involves polymer chains complexed with the SWNT in the isotactic composite. The increase in the glass transition temperature and the change in heat capacity suggest that the isotactic polystyrene is better able to interact with the surface of the SWNT. Therefore, both computational and experimental results suggest that the isotactic polystyrene is more effective in interacting with the SWNT and thus better capable of dispersing the SWNT within the polymer matrix compared with the atactic polystyrene.

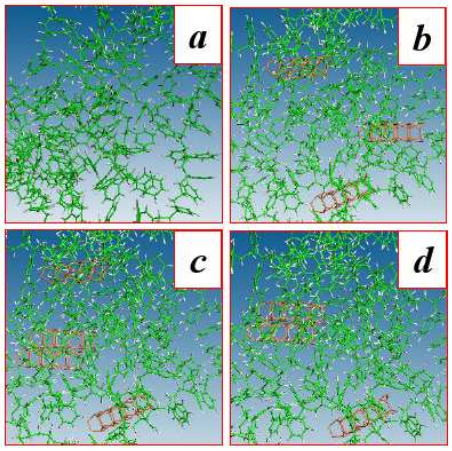

Scheme 1. Illustration of the dispersion mechanism of SWNT into the polymer matrices.

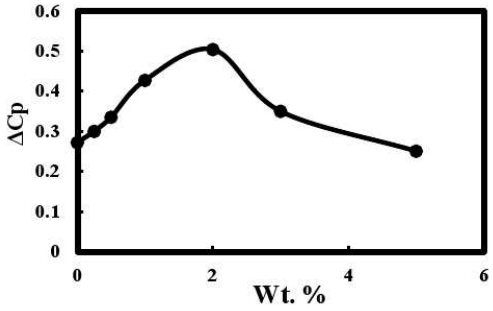

Figure 6. The ΔC_p of isotactic polystyrene/SWNT nanocomposite as a function of nanotube content.

Solution and Solid State NMR studies

The band structures for the isotactic and the atactic polystyrene wrapped SWNT are shown in Figure 7. The computational results show that the phenyl group of the polystyrene acts as a donor, and such donation should results in a decrease in the π-electron density of the aromatic ring. The decrease in the π-electron density may result in deshielding of the aromatic protons as the aromatic protons shift downfield.[52] Computational studies suggest charge transfer interactions between the polymers with the SWNT. As seen in Figure 7, there exist dispersed and flat bands in the calculated band structure. The flat bands represent the non-interacted (non-dispersed) polystyrene polymer molecular levels that align SWNT. As a result of the charge transfer from the polymer to

the SWNT, flat bands near the Fermi level disperse. In the isotactic band structure (Figure 7), the flat band has lower energy than the atactic band structure. The flat band regions are highlighted by brackets in Figure 7. The alignment of flat bands relative to the Fermi level indicates that there are more polymer molecular levels interacting with SWNT in isotactic polystyrene compared to atactic polystyrene. The isotactic polymer is a better charge donor to the SWNT compared to the atactic polymer. It was shown earlier that in a poly (2-methoxystyrene)/graphene composite, the polymer backbone serves as charge donors to graphene, resulting in the doping of graphene.[53] The distinctive doping behaviour between atactic and isotactic polymers is thus of importance to the relative interaction strength with SWNTs.

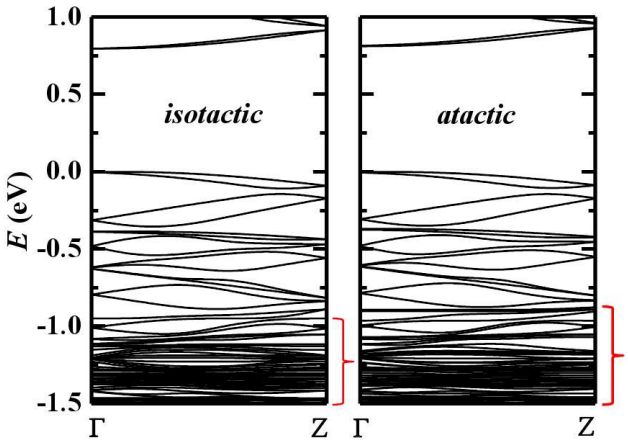

Figure 7. Calculated band structures for (a) *isotactic*-polystyrene wrapped SWNT, (b) *atactic*-polystyrene wrapped SWNT. Γ = 0 and Z = $\pi/2a$, where a = 47.5 Å. The valence band maximum is set to 0 eV. Brackets indicate the flat band regions of the band structure.

The 500 MHz ^{1}H-NMR spectra of a SWNT-polymer chloroform (deuterated) solutions show changes in chemical shifts as a function of increasing SWNT. The observed changes in chemical shift as a function of SWNT are shown in Figure 8. The change in chemical shifts (δ) was detected with respect to the chloroform peak at 7.29 ppm. As the SWNT content is increased in the isotactic polystyrene solution, a slight downfield movement of the aromatic protons is initially observed. However, when the SWNT content is increased to 1%, the chemical shift moves upfield. Figure 8 also shows a similar plot for the atactic polymer, which only shows upfield chemical shifts. The downfield shift of the isotactic polymer is fairly small but these are in the solution state spectra in which association and dissociation of the polymer and the SWNT take place. The fact that a downfield shift is observed even in solution suggests that isotactic polystyrene is better able to complex with the SWNT and act as a charge donor. The downfield shift reaches a maximum at around 0.5% SWNT. It is interesting to note that at 1% SWNT content, both the isotactic and the atactic polymers show the same upfield chemical shift. When the capacity of the isotactic polymer is saturated, any additional SWNT will agglomerate and the two systems will become quite similar in that the majority of the SWNT are in the agglomerated form even in the solution state.

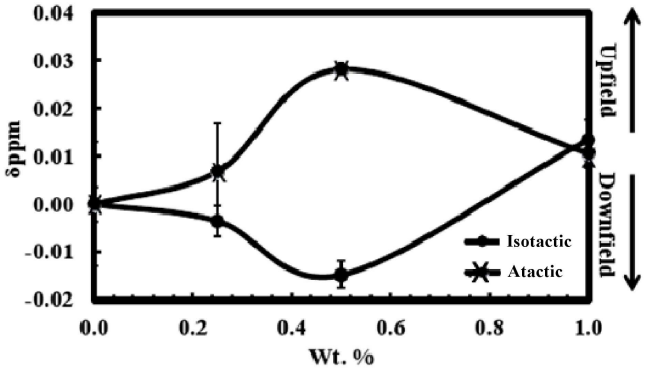

Figure 8. Change in chemical shift (δ) for the aromatic protons of polystyrene as a function of SWNT content.

Rotating frame ^{13}C $T_{1\rho}$ relaxation rates of the polystyrene/SWNT matrices complements the computational, thermal (DSC) and solution NMR studies. The ^{13}C $T_{1\rho}$ relaxation rates are listed in Table 4. The reported $T_{1\rho}$ is the highest $T_{1\rho}$ for each of the system and one can reasonably conclude the $T_{1\rho}$ corresponds to the higher Tg. The ^{13}C $T_{1\rho}$ rates of the isotactic polymer increases on increasing the SWNT content. The increase in the relaxation rateis most likely due to the formation of the non-covalent crosslinking in the isotactic polystyrene/SWNT matrix and is consistent with the increase in the glass transition temperature observed on increasing SWNT in the matrix (Table 3). Therefore, the rotating frame ^{13}C $T_{1\rho}$ spin lattice relaxation rates support the formation of the Type-B matrix shown in Scheme 1. The decrease in the rotating frame ^{13}C $T_{1\rho}$ relaxation rates for the atactic polystyrene/SWNT matrix also complements the initial decrease in the glass transition temperature observed for the system. Both the decrease in the relaxation rates and lowering of the glass transition temperature suggest that the segmental motion of the chains increase with addition of low amount of SWNT to the atactic polystyrene i.e. a plasticization effect is taking place.

Table 4. ^{13}C $T_{1\rho}$ relaxation rates of isotactic and atactic polystyrene/SWNT composites

% SWNT	Atactic [ms]	Isotactic [ms]
0	2.50	2.15
0.25	2.10	2.19
0.5	2.09	2.26
1	1.60	2.43

Computational, thermal (T_g and change in heat capacity), solution and solid state NMR results strongly suggest that the isotactic polystyrene is better in dispersing SWNT within its matrix compared with the atactic polymer.

Conclusions

Our results demonstrate that stereoregularity of polystyrene plays an important role in the capacity of the polystyrene to interact with the SWNT surface. Both computational modeling and experimental studies strongly suggest that the isotactic polystyrene is more effective in interacting with the SWNT compared to the atactic polystyrene. At low SWNT contents (< 0.5%), the SWNT is well dispersed within the isotactic polystyrene and forms a non-covalent crosslinked matrix. Because of the formation of the non-covalent crosslinked matrix, the glass transition temperature of the isotactic polymer increases with increasing SWNT content. At low SWNT contents, the isotactic polystyrene/SWNT matrix can be depicted as Type B matrix. On the other hand, even at low SWNT contents (0.5%), the atactic polystyrene/SWNT matrix may be depicted by Type D matrix where the SWNT forms agglomerates since the interaction between the atactic polymer and SWNT is not as effective. Our findings pave the way that dispersion of SWNTs within a polymer matrix can be accomplished by using the same polymer but with different stereoregularity.

Acknowledgements

This work was supported by National Science Foundation (DMR-0934142 and HRD-1137751) and Army Research Office (W911NF-12-1-0048).

Notes and References

[a]Department of Chemistry and Center for Functional Nanoscale Materials, Clark Atlanta University, 223 James P. Brawley Dr., Atlanta, GA 30314, United States.
[b]Department of Physics and Center for Functional Nanoscale Materials, Clark Atlanta University, 223 James P. Brawley Dr., Atlanta, GA 30314, United States. *Email: xwang@cau.edu

1. H. Kim, A. A. Abdala, C. W. Macosk, *Macromolecules* 2010, ***43***, 6515-6530.
2. R. A. Vaia, J. F. Maguire, *Chem. Mater.* 2007, ***19***, 2736-2751.
3. R. Benmouna, M. J. Benmouna, *Chem. Eng. Data* 2010, ***55***, 1759-1767.
4. K. Chen, K. Harris, S. Vyazovkin, *Macromol. Chem. Phys.* 2007, ***208***, 2525-2532.
5. R. R. Eckman, P. M. Henrichs, A. J. Peacock, *J. Macromolecules* 1997, ***30***, 2474-2481.
6. R. Andrews, M. C. Weisenberger, *Current Opinion in Solid State and Materials Science* 2003, **8**, 31-37.
7. M. J. Biercuk, M. C. Llaguno, M. Radosavljevic, J. K. Hyun, A. T. Johnson, *Appl. Phys. Lett.* 2002, **80**, 2767-2769.
8. J. M. Bell, R. G. S. Goh, E. R. Waclawik, M. Giulianini, N. Motta, *Materials Forum* 2008, **32**, 144-152.
9. M. Chipara, J. Cruz, E. R. Vega, J. Alarcon, T. Mion, D. M. Chipara, E. Ibrahim, S. C. Tidrow, D. Hui, *Journal of Nanomaterials* 2012, **12**, 1-6.
10. M. N. Tchoul, W. T. Ford, M. L. P. Ha, I. Chavez-Sumarriva, B. P. Grady, G. Lolli, D. E. Resasco, S. Arepalli, *Chem. Mater.* 2008, ***20***, 3120-3126.
11. R. Shenhar, T. B. Norsten, V. M. Rotello, *Adv. Mater.*, 2005, **17**, 657-669.
12. G. Schmidth, M. M. Malwitz, Current Opinion in Colloid and Interface Science 2003, **8**, 103-108.
13. S. Kumar, T. Rath, R. N. Mahaling, and C. K. Das, *Composites Part A: Applied Science and Manufacturing* 2007, **38**, 1304-1317.
14. S. Wang, M. Tambraparni, J. Qiu, J. Tipton, and D. Dean, *Macromolecules* 2009 **42**, 5251- 5255.
15. M. Abdalla, D. Dean, P. Robinson, E. Nyairo, *Polymer* 2008 **49**, 3310-3317.
16. A. Guiseppi-Elie, C. Lei and R. Baughman, Nanotechnology 2002 **13**, 559-564.
17. Y. N. Pandey, G. J. Papakonstantopoulus, M. Doxastakis, *Macromolecules* 2013, **46**, 5097-5106.
18. P. Rittigstein, J. M. Torkelson, *J. Polym. Sci. Part B: Poly. Phys.* 2006, **44**, 2935.2943.
19. J. S. Smith, D. Bedrov, G. D. Smith, *Compos. Sci. Technol.* 2003, **63**, 1599-1605.
20. G. D. Smith, D. Bedrov, *Langmuir* 2009, **25**, 11239-11243.
21. J. Oberdisse, *Soft Matter* 2006, **2**, 29-36.
22. A. Moisala, Q. Li, I. A. Kinloch, A. H. Windle, *Compos. Sci. Technol.* 2006, **66**, 1285-1288.
23. E. Tamburri, S. Orlanducci, M. C. Terranova, F. Valentini, G. Palleschi, A. Curulli, F. Brunetti, D. Passeri, A. Alippi, M. Rossi, *Carbon* 2005, **43**, 1213-1221.
24. W. Bauhofer, J. Z. Kovacs, *Compos. Sci. Technol.* 2009, **69**, 1486-1498.
25. I. Szleifer, R. Yerushalmi-Rozen, *Polymer* 2005, **46**, 7803-7818.
26. D. Bikiaris, *Materials* 2010, **3**, 2884-2946.
27. I. Alig, D. Lellinger, M. Engel, T. Skipa, P. Potschke *Polymer* 2008, **49**, 1902-1909.
28. A. Shaw, S. Sriramula, P. D. Gosling, M. K. Chryssanthopoulo, *Composites Part B* 2010, **41**, 446-453.
29. O. Karunwi and A. Guiseppi-Elie *J. Nanobiotechnology* 2013, **11**, 6.
30. Y. Zhang, K. Song, J. S. Meng, and M. L. Minus, *ACS Applied Materials & Interfaces,* 2013, **13**, 807-814.
31. M. P. Stevens, *Polymer Chemistry: An Introduction.* 3rd Ed.; Oxford University Press: New York, 1998**.**
32. J. M. Guenet, C. Picot, H. Benoit, *Macromolecules* 1979, **12**, 86-90.
33. E. D. T. Atkins, A. Keller, J. S. Shapiro, P. J. Lemstra, *Polymer* 1981, **22**, 1161-1164.
34. T. Nakaoki, M. J. Kobayashi, *J. Mol. Struct.* 2003, **655**, 343-349.
35. A. M. Shammgharaj, J. H. Bae, R. R. Nayak, S. H. Ryu, *J. Polym. Sci. Part A: Polym. Chem.* 2007, **45**, 460-470.
36. C. Stephan, T. P. Nguyen, M. Lamy de la Chapelle, S. Lefrant, C. Journet, P. Bernier, *Synthetic Metals* 2000, **108**, 139-149.
37. T. Hanemann, D. V. Szabo, *Materials* 2010, ***3***, 3468-3517.
38. B. P. Grady, A. Paul, J. E. Peters, W. T. Ford, *Macromolecules* 2009, **42**, 6152-6158.
39. P. R. Sundararajan, N. Tyrer, *Polymer* 1981, **6**, 359-366.
40. M. N. Tchoul, W. T. Ford, G. Lolli, D. E. Resasco, S. Arepalli, *Chem. Mater.* 2007, **19**, 5765-5772.
41. Materials Studio, *Accelrys Material Studio*, 5.5; Accelrys Software Inc.: San Diego, CA.
42. Y. Chen, X. Xu, Q. Wang, R. Gunasinghe, X. Q. Wang, Y. Pang, *Small* 2013, **9**, 870-875.
43. O.O. Ogunro, X. Q. Wang, *Nano Lett.* 2009, **9**, 1034-1038.
44. O. O Ogunro, K. Karunwi, I. M. Khan, X. Q. Wang, *J. Phys .Chem. Lett.* 2010, **1**, 704-707.
45. Y. K. Kang, O. S. Lee, P. Deria, S. H. Kim, T. H. Park, D. A. Bonnell, J. G. Saven, M. J. Therien, *Nano Lett.* 2009, **9**, 1414-1418.
46. C. L. Huang, Y. C. Chen, T. J. Hsiao, J. C. Tsai, C. Wang, *Macromolecules* 2011, **44**, 6155-6161.
47. F. A. Bovey, P. Mirau, *NMR of Polymers*. 1st Ed.; Elsevier Science and Technology, 1996.
48. N. Grossiord, H. E. Miltner J. Loos, J. Meuldijk, B. V. Mele, C. E. Koning, *Chem. Mater.* 2007, **19**, 3787-3792.
49. J. Li, I. M. Khan, *Macromolecules* 1993, **26**, 4544-4550.
50. J. Li, L. M. Pratt, I. M. Khan, *J. Polym. Sci. Poly Chem. Ed.* 1995, **33**, 1657-1663.
51. D. R. Paul, L. M. Robeson, *Polymer* 2008, **49**, 3187-3204.
52. E. Powell, Y-H. Lee, R. Partch, D. Dennis, T. Moreg, M. Varshney, *Int. J. Nanomedicine* 2007, **3**, 449-459.
53. D. Reuven, K. Suggs, M. D. Williams, X.-Q. Wang, *ACS Nano* 2012, **6**, 1011-1017.

